EUROPHYSICS LETTERS 1 November 2005

*Europhys. Lett.*, **72** (3), pp. 479–485 (2005)
DOI: 10.1209/epl/i2005-10249-1

# From ferro- to antiferromagnetism via exchange-striction of MnAs/GaAs(001)

H. Yamaguchi(*), A. K. Das(**), A. Ney(***), T. Hesjedal, C. Pampuch(*), D. M. Schaadt and R. Koch(*)

*Paul-Drude-Institut für Festkörperelektronik - Hausvogteiplatz 5-7*
*D-10117 Berlin, Germany*

received 22 July 2005; accepted in final form 8 September 2005
published online 30 September 2005

PACS. 75.70.Ak – Magnetic properties of monolayers and thin films.
PACS. 68.60.Bs – Mechanical and acoustical properties.
PACS. 75.80.+q – Magnetomechanical and magnetoelectric effects, magnetostriction.

**Abstract.** – We investigated the stress evolution in single-crystal MnAs films on GaAs(001) upon applying high external magnetic fields in the $\alpha/\beta$ phase transition regime (10–40 °C) and beyond. Our stress measurements reveal large field-induced lattice distortions at temperatures, where $\beta$-MnAs is present, even well above the phase transition ($> 40$ °C). A quantitative comparison with the field-induced increase of magnetization reveals that the changes in the lattice dimensions can be fully explained by the (reversible) back-transformation of $\beta$-MnAs to $\alpha$-MnAs. Our direction-dependent experiments identify the structural distortions at the phase transition as a volume magnetostriction effect and —due to the persisting magnetocrystalline anisotropy above 40 °C— strongly support an antiferromagnetic state for $\beta$-MnAs.

Manganese arsenide, though it was discovered by Heusler in the early 1900s [1], is attracting considerable attention in the recent years. It was found that its ferromagnetic $\alpha$-phase is one of the few ferromagnetic compounds that are compatible with the technologically leading semiconductor surfaces Si(001) and GaAs(001) [2–4]. In addition, the quite unique magnetic properties make MnAs also very interesting from a fundamental point of view.

The ferromagnetic $\alpha$-MnAs phase crystallizes in the hexagonal NiAs structure which exhibits alternating hexagonal planes of Mn and As atoms (see fig. 1a). In the bulk, $\alpha$-MnAs is stable up to a temperature of about 40 °C, at which it transforms into the quasi-hexagonal (orthorhombic) $\beta$-MnAs by a first-order phase transition [5–7]. The lattice spacing of the hexagonal plane ($a$-axis) abruptly shrinks by $\sim 1.0\%$ and ferromagnetic order breaks down in a discontinuous manner. Surprisingly, the Mn-Mn distance along the $c$-axis, where the Mn atoms are nearest neighbors, remains unchanged during coupled structural and magnetic phase transition. In the case of MnAs films, the $\alpha/\beta$ phase transition is modified by the epitaxial constraints imposed by the substrate. For instance, the phase transition of MnAs/GaAs(001)

(*) Permanent address: NTT Basic Research Laboratories - 3-1 Morinosato Wakamiya, Atsugi-shi, Kanagawa 243-0198, Japan.
(**) New address: Department of Physics and Meteorology, Indian Institute of Technology - Kharagpur-721302, India.
(***) New address: Fachbereich Physik, Universität Duisburg-Essen - Lotharstrasse 1, 47048 Duisburg Germany.
(*) New address: Specs GmbH - Voltastraße 5, 13355 Berlin, Germany.
(*) E-mail: koch@pdi-berlin.de

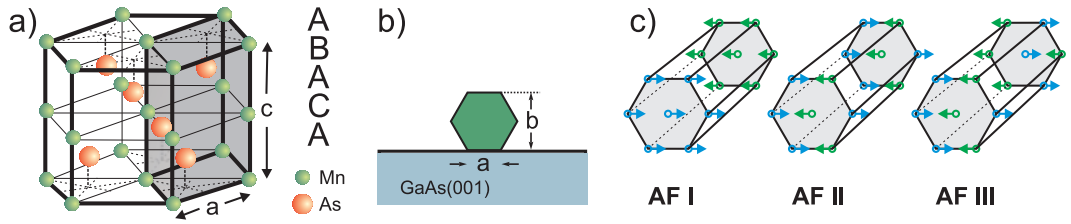


Fig. 1 – a) NiAs-type crystal structure of $\alpha$-MnAs consisting of hexagonal planes of Mn and As alternating in a sequence ABAC. b) Epitaxial configuration of MnAs/GaAs(001) with the $a$- and $c$-axes of MnAs oriented parallel to GaAs[110] and GaAs[1$\bar{1}$0], respectively. c) Antiferromagnetic models of $\beta$-MnAs used for the DFT calculations in ref. [16]; arrows indicate the magnetic moment of Mn.

no longer proceeds abruptly as in the bulk [8]. Instead, a regular pattern of alternating $\alpha$- and $\beta$-MnAs stripes extending along the $c$-axis is stabilized by strain in the broad temperature range 10–40 °C [9, 10]. In the phase coexistence regime the magnetization continuously decreases [11], but —as is revealed by a comparison with X-ray diffraction data [10]— this is mainly due to the decrease of the ferromagnetic $\alpha$-MnAs fraction; the phase transition itself remains first order [12].

An important but still controversially discussed topic concerns the magnetic structure of $\beta$-MnAs. Already Guillaud [13] presumed that the Curie temperature ($T_C$) is not at the $\alpha/\beta$ phase transition ($T_{crit}$); extrapolation of the temperature dependence of the spontaneous magnetization suggests a disappearance of ferromagnetic order at about 130 °C, *i.e.*, at the temperature where orthorhombic $\beta$-MnAs transforms into the hexagonal, paramagnetic $\gamma$-phase [5]. This fact, and the anomalous behavior of the susceptibility of $\beta$-MnAs (*i.e.*, between 40 and 130 °C) led to the speculation that $\beta$-MnAs is antiferromagnetic [13,14]. However, no long-range order was detected by neutron diffraction [15]. Very recently, the discussion was revived by a density functional theory (DFT) study of $\beta$-MnAs performed by Niranjan *et al.* [16], which clearly discards a paramagnetic $\beta$-MnAs and strongly supports an antiferromagnetic state with lacking long-range order (see fig. 1c).

Here we report on the stress evolution in single-crystalline MnAs films on GaAs(001) at the $\alpha/\beta$ phase transition, when high external magnetic fields are applied. Our stress measurements reveal large field-induced lattice distortions at temperatures where $\beta$-MnAs is present, even well above $T_{crit}$. A quantitative comparison with the field-induced increase of magnetization, detected by SQUID (superconducting quantum interference device) magnetometry, reveals that the changes in the lattice dimensions can be fully explained by the (reversible) back-transformation of $\beta$-MnAs to $\alpha$-MnAs. From the involved energy contributions we identify the structural distortions at the phase transition as a volume magnetostriction effect, driven by the gain in exchange energy. The persisting magnetocrystalline anisotropy above $T_{crit}$ as well as the direction-dependence of the lattice distortions strongly support an antiferromagnetic state for $\beta$-MnAs (see fig. 1c).

The measurements were performed on 60-nm-thick, high-quality single-crystal MnAs films on GaAs(001). The films were prepared by molecular beam epitaxy on commercial, 100-$\mu$m-thick, epiready GaAs(001) wafers as described in detail elsewhere [17, 18]. Under the chosen conditions, MnAs grows predominantly in its A-orientation (see Fig. 1b) with the MnAs($\bar{1}$100) plane parallel to the substrate surface and MnAs[0001] $\parallel$ GaAs[1$\bar{1}$0] [19]. The film contains only small amounts of MnAs in the B-orientation (rotated by 90 ° in-plane) [19] as well as a small fraction with an out-of-plane magnetization [20]. The magnetic measurements were performed with a sensitive cantilever beam magnetometer (CBM) [21] using 25×5 mm$^2$

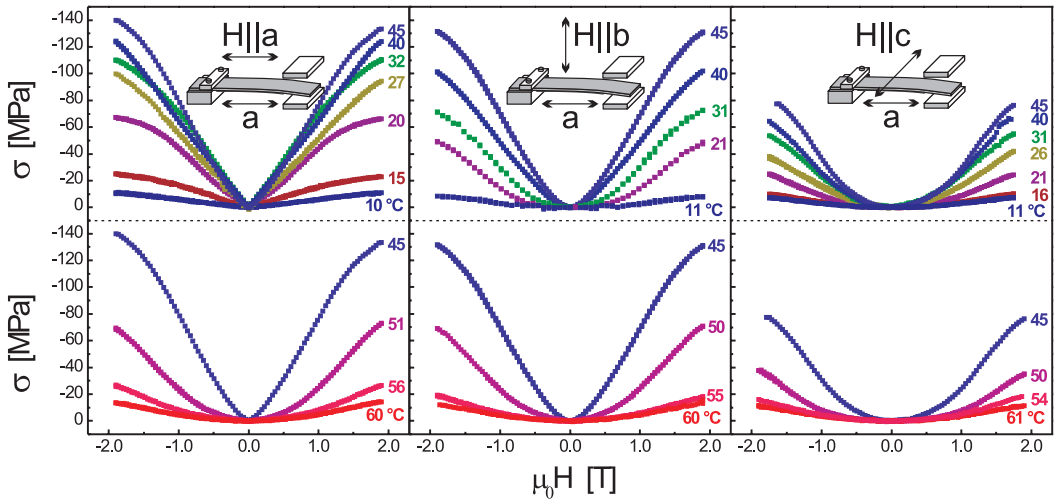


Fig. 2 – Stress evolution in 60 nm MnAs/GaAs(001) at different temperatures, induced by an external magnetic field ($H$) parallel to the $a$-, $b$-, and $c$-axes of MnAs, respectively; each data point is obtained from the change in substrate deflection with and without magnetic field; upper and lower diagrams display the results at temperatures below and above zero-field $T_{\mathrm{crit}}$, respectively. For $H \| b$ the torque $\vec{T} = \mu_0 \vec{M} \times \vec{H}$ was determined by the procedure described in ref. [22] and subtracted from the curves measured at 10–40 °C; we did not correct the $H \| a$ curve for the small torque effect due to the out-of-plane magnetization; B-oriented MnAs leads to negligible stress contributions (∼1%); the small asymmetry observed in some stress curves is due to thermal drift.

substrates with GaAs[110] or GaAs[1$\bar{1}$0] along the length and the film covering an area of 11 × 5 mm$^2$. The film magnetization up to magnetic fields of 5 T was determined by a commercial SQUID magnetometer.

Figure 2 displays the stress developing in the MnAs film when the magnetic field ($H$) is applied parallel to the $a$-, $b$- and $c$-axes at different temperatures. Each data point is obtained from the change in substrate deflection with and without applied magnetic field, thus demonstrating the full reversibility of the field-induced stress. The experimental geometry of the latter two series actually is employed in magnetostriction ($\lambda$) measurements with a CBM, where the change of the equilibrium lattice spacings upon varying the film magnetization gives rise to magnetostrictive stress (here by rotating the film magnetization ($M$) from the easy $a$-axis to the $b$- or $c$-axes, respectively). In accordance with a recent study [23], the magnetostrictive stress of the pure $\alpha$-phase (*i.e.*, at 10 °C in fig. 2) is small, yielding magnetoelastic coupling constants of the same order of magnitude as for the transition metals Fe, Co, and Ni. In the phase coexistence regime (10–40 °C), on the contrary, the field-induced stress increases by more than one order of magnitude and interestingly becomes the larger the smaller the $\alpha$-MnAs fraction. Large field-induced stress is observed even above the phase transition temperature ($T > 40$ °C) and is still detectable at 60 °C (see lower diagrams of fig. 2). Surprisingly, a comparable stress change is observed also for $H$ parallel to $a$ in the film plane, which is the easy magnetization axis of MnAs/GaAs(001). In this experimental geometry no magnetostrictive stress can be measured, because the magnetization of individual domains is oriented parallel to $a$ with and without magnetic field, the latter serving as the reference stress (note that $\lambda \propto M^2$, thus independent of the sign of $M$). Our measurements therefore suggest that the observed field-induced stress is directly related to the $\alpha/\beta$ phase transition.

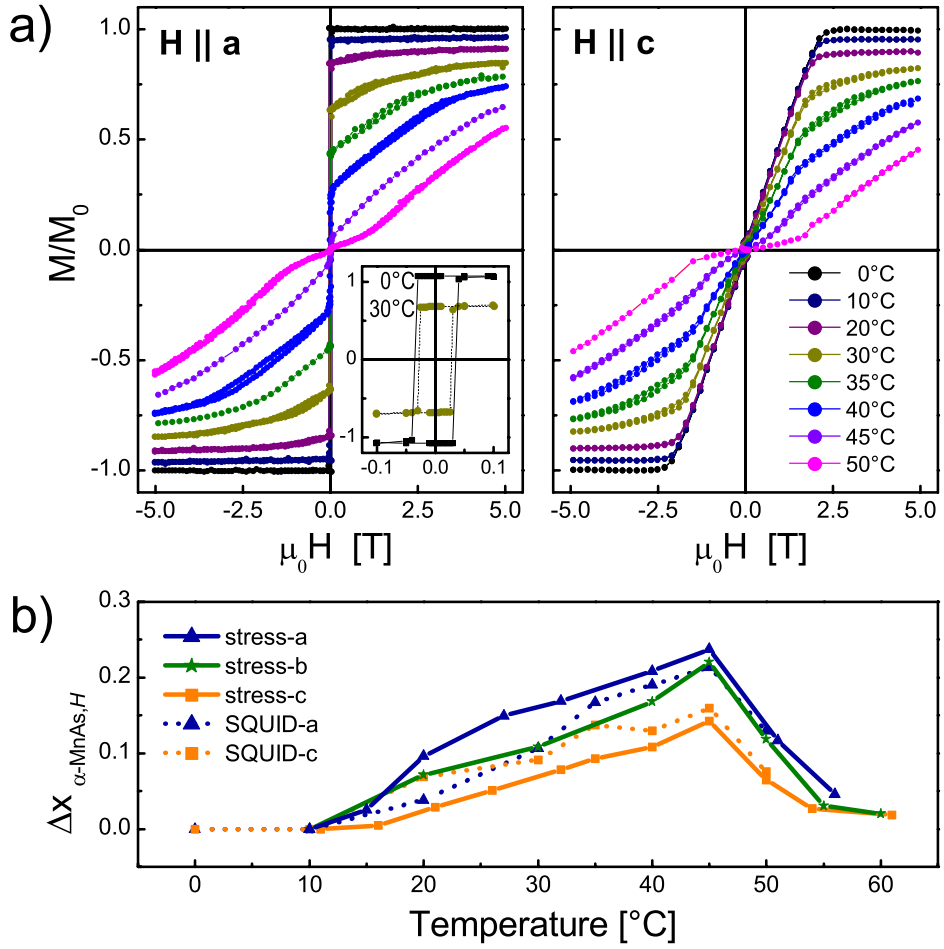


Fig. 3 – a) Normalized magnetization $M/M_0$ of MnAs/GaAs(001) determined by SQUID at different temperatures with the magnetic field $H$ applied parallel to the $a$- and $c$-axes; $M_0$ is the magnetization at 0 °C (0.67 MA/m [11]); the inset shows the magnified square hysteresis loops at 0 and 30 °C, which are observed at small magnetic fields and indicate magnetic saturation of the $\alpha$-MnAs fraction along the easy $a$-axis. b) Comparison of the field-induced $\alpha$-MnAs fraction $\Delta x_{\alpha\text{-MnAs},H}$ calculated from the SQUID data and the magnetostrictive stress of fig. 2 for $\mu_0 H = 1.9$ T.

Further insight is provided by SQUID measurements (fig. 3a). In agreement with previous studies (*e.g.*, [11]), square hysteresis loops are observed when small magnetic fields are applied parallel to the easy $a$-axis in the film the plane (the inset of fig. 3a, left, shows magnified hysteresis curves at 0 and 30 °C). Obviously the $\alpha$-MnAs fraction is magnetically saturated already at small magnetic fields as confirmed by magnetic force microscopy (see ref. [11]). However, at temperatures where $\beta$-MnAs is already present (>10 °C), the magnetization increases in higher fields, thus indicating the formation of additional $\alpha$-MnAs from $\beta$-MnAs. We used the SQUID data of fig. 3a, left, to calculate the additional $\alpha$-MnAs fraction $\Delta x_{\alpha\text{-MnAs,H}}$ from the field-induced gain in magnetization (fig. 3b) at 1.9 T. Since all of the converted $\alpha$-MnAs is most likely also magnetized by the applied magnetic field —particularly above $T_{\text{crit}}$— we assumed the value at 0 K for the magnetic moment of $\alpha$-MnAs (0.88 MA/m [24]).

The field-induced $\alpha$-MnAs fraction obtained from the SQUID data with $H\|a$ (blue on-line, dashed/triangle curve in fig. 3b) is in very good agreement with the $\alpha$-MnAs fraction calculated from the stress data of fig. 2 with $H\|a$ and $H\|b$ (blue on-line, solid/triangle and green on-line, solid/asterisk curves, respectively); we used the conversion factor of 0.59 GPa determined in ref. [11] for the complete transformation of $\beta$-MnAs into $\alpha$-MnAs. Note that at 45 °C, *i.e.*, above $T_{\mathrm{crit}}$, an additional $\alpha$-MnAs fraction of $\sim$25% is recovered. Figure 3a, right, displays SQUID measurements with the magnetizing field parallel to the hard $c$-axis. Whereas at 0–10 °C the films are magnetically saturated for $\mu_0 H > 2.2$ T, in the phase coexistence regime the magnetization further increases at high magnetic fields. Taking the $\alpha$-MnAs fraction at zero field from the SQUID data with $H\|a$ and assuming that 91% are magnetized along $c$ at 1.9 T (according to the SQUID data of fig. 2a, right), we obtain the orange on-line, dashed/square SQUID curve of fig. 3b for the field-induced $\alpha$-MnAs fraction with $H\|c$. Again this curve is in very good agreement with the respective stress data (orange on-line, solid/square curve). Note also the finite slope of the stress curves below 40 °C in the case of $H\|a$ and $H\|b$ for $H \to 0$, which indicates that the back-transformation of $\beta$-MnAs is facilitated when $\alpha$-MnAs stripes are already present.

From our combined stress and SQUID results it can be concluded that the entire stress evolving during the reversible field-induced transformation of $\beta$-MnAs into $\alpha$-MnAs originates from the change in the equilibrium lattice spacings due to the structural phase transition. No additional magnetostrictive effects are involved. A field-induced structural transformation was recently also found in bulk samples of MnAs [25–27], where at 50 °C, *i.e.*, 10 °C above the phase-transition temperature, and magnetic fields of $\sim$5 T a complete conversion of $\beta$-MnAs into $\alpha$-MnAs is achieved.

Due to the heteroepitaxial constraints in MnAs/GaAs(001), where the Zeeman energy ($E_{\mathrm{Z}} = \mu_0 H M = 0.35$ meV per Mn with $M = 0.88$ MA/m and $\mu_0 H = 1.9$ T) has to compete also with the elastic energy ($E_{\mathrm{el}} = c_{11}\varepsilon_1^2/2 = 0.43$ meV/Mn using the elastic constant $c_{11}$ from ref. [28] and strain $\varepsilon_1 = 1.0\%$), magnetic fields of 5 T are not sufficient for a complete structural conversion. Above 40 °C the amount of the back-transformation is almost identical for $H\|a$ and $H\|b$ (see fig. 2). This finding is consistent with the isotropy of the magnetocrystalline energy in the hexagonal plane [29] and an isotropic shape anisotropy (note that in both cases probably spherical clusters are nucleating above $T_{\mathrm{crit}}$). For $H\|c$ the magnetocrystalline energy of 0.15 meV/MnAs [29] is about half of the Zeeman energy, which explains the observed reduction of the field-induced $\alpha$-MnAs fraction compared with the other geometries. We remark that the magnetoelastic energy of 0.027 meV calculated with the coupling constants of $\alpha$-MnAs [23] plays only a minor role. Obviously, the anisotropy observed by our direction-dependent experiments is the result of the magnetocrystalline anisotropy of $\alpha$-MnAs. Since for common ferromagnets anisotropic behavior disappears at $T_{\mathrm{C}}$, our study provides additional experimental support that $T_{\mathrm{crit}}$ of MnAs is not a Curie temperature.

After these energetic considerations we want to address the question of the driving force of the coupled structural and magnetic phase transition. Is it a) the gain in the exchange energy or b) the lowering of the "bonding" energy, which we define here as the change in energy due to the varying dimensions and symmetry of the crystal lattice apart from the exchange energy? The "bonding" energy can be estimated from the elastic energy, since the involved lattice distortions, though being $\sim$1%, are still small enough to use first-order elasticity. This means that the change in "bonding" energy during the phase transition is of the order of 0.5 meV/Mn (see above). A first estimate for the exchange energy (see also the discussion below) is provided by the mean-field theory with $E_{\mathrm{ex}} \sim 0.5 k_{\mathrm{B}} T_{\mathrm{C}}$. With the Curie temperature $T_{\mathrm{C}}$ lying between 40 and 130 °C, values of 13–17 meV/Mn are obtained for the exchange energy, which are considerably higher than $E_{\mathrm{el}}$ and, moreover, of the same order of magnitude as the

latent heat of MnAs (9.8 meV/Mn from ref. [30]). Our experiments therefore provide strong evidence that the $\alpha/\beta$ phase transition is driven by the gain in exchange energy, thus implying that the involved lattice distortions are of magnetic origin and can be regarded as a volume magnetostriction effect. We want to remark that this conclusion is not contradictory to our previous study [11], where we excluded "exchange magnetostriction" in the sense of a varying Mn-Mn distance along the $c$-axis in favor of an indirect exchange mechanism.

In view of the magnetocrystalline anisotropy, which we detected by our direction-dependent experiments at $T_{\rm crit}$ and which contradicts a phase transition from a ferromagnetic to an *isotropic* paramagnetic state, it is worth discussing what we can learn from our experiments about the magnetic state of $\beta$-MnAs. As mentioned above, the DFT study of Niranjan *et al.* [16] strongly favors an antiferromagnetic $\beta$-MnAs. In that study the three antiferromagnetic models of fig. 1c were considered, which due to a lack of long-range order are hardly detected by neutron scattering. Their cohesive energies are about 400 meV lower than that of the paramagnetic state, with models AF II and AF III lying an additional 40 and 41 meV below model AF I. Aside from the anomalous susceptibility of $\beta$-MnAs, which is inconsistent with a paramagnetic ground state, there comes further experimental support from the specific changes in the lattice dimensions of MnAs at its phase transitions. It is certainly astonishing that at the $\alpha/\beta$ phase transition only the length of $a$ changes, whereas $c$ remains constant. In fact, this finding clearly excludes model AF I, where the hexagonal planes of Mn are ferromagnetic but oppositely polarized from plane to plane. For this model mainly the ferromagnetic coupling along the $c$-axis has to be broken, which also in the case of an indirect exchange mechanism should be accompanied by a small change of the $c$-spacing. We remark that the same structural behavior is found also for the field-induced transition. Using substrates with the $c$-axis of MnAs parallel to the length we observe only a very small stress change (not shown here). It is $\sim$12% of that in fig. 2 and opposite in sign, thus indicating that the Poisson effect of the stress along $a$ is measured; the experimental value is within the error bars of the estimated Poisson effect of (22$\pm$13)% ($\Delta\sigma_3/\Delta\sigma_1 \approx c_{13}/(c_{11}+c_{12})$ using the $c_{ij}$ from ref. [28]). For model AF III there is antiferromagnetic ordering within and between the hexagonal Mn planes, which should result in length changes of $a$ and $c$ at the $\alpha/\beta$ phase transition. Only model AF II with antiferromagnetic order within the hexagonal Mn planes and ferromagnetic order between them is consistent with the structural properties, *i.e.*, change of $a$ but no change of $c$ at the $\alpha/\beta$ phase transition along with a change of $c$ at the $\beta/\gamma$ phase transition [5] when MnAs becomes paramagnetic and the ferromagnetic order along the $c$-axis is lifted. It is noteworthy that ferromagnetic ordering along $c$ cannot be detected by neutron scattering in polycrystalline samples [15].

In conclusion, our study provides important new insight for an understanding of the magnetic behavior of MnAs: i) The combined CBM and SQUID experiments reveal that the field-induced lattice distortion can be explained fully by the structural transformation at the $\alpha/\beta$ phase transition. ii) The structural transformation is driven by the gain in exchange energy, thus supporting the "exchange-striction" concept proposed for MnAs by Kittel in 1960 [14]. iii) With our direction-dependent experiments on a single-crystal sample we detected a magnetocrystalline anisotropy at $T_{\rm crit}$, which is not consistent with a phase transition from a ferromagnetic to an isotropic paramagnetic state. iv) The observed direction dependence of the lattice distortions strongly support an antiferromagnetic $\beta$-MnAs, namely model AF II of ref. [16] (fig. 1c).

* * *

We thank L. Däweritz for providing MnAs samples, C. Herrmann and M. Kästner for sample preparation, K. H. Ploog for stimulating discussions and M. Bowen for critically reading the manuscript.

REFERENCES


[1] Heusler F., *Z. Angew. Chem.*, **17** (1904) 260.
[2] Tanaka M., Harbison J. P., Park M. C., Park Y. S., Shin T. and Rothberg G. M., *J. Appl. Phys.*, **76** (1994) 6278.
[3] Tanaka M., *Physica E*, **2** (1998) 372.
[4] Schippan F., Däweritz L., Behme G., Ploog K. H., Dennis B., Neumann K. -U. and Ziebeck K. R. A., *J. Appl. Phys.*, **88** (2000) 2766.
[5] Willis B. T. M. and Rooksby H. P., *Proc. Phys. Soc. (London) B*, **67** (1954) 290.
[6] Bean C. P. and Rodbell D. S., *Phys. Rev.*, **126** (1962) 104.
[7] Wilson R. H. and Kasper J. S., *Acta Cryst.*, **17** (1964) 95.
[8] Kaganer V. M., Jenichen B., Schippan F., Braun W., Däweritz L. and Ploog K. H., *Phys. Rev. Lett.*, **85** (2000) 341.
[9] Plake T., Ramsteiner M., Kaganer V. M., Jenichen B., Kästner M., Däweritz L. and Ploog K. H., *Appl. Phys. Lett.*, **80** (2002) 2523.
[10] Kaganer V. M., Jenichen B., Schippan F., Braun W., Däweritz L. and Ploog K. H., *Phys. Rev. B*, **66** (2002) 045305.
[11] Das A. K., Pampuch C., Ney A., Hesjedal T., Däweritz L., Koch R. and Ploog K. H., *Phys. Rev. Lett.*, **91** (2003) 087203.
[12] Ney A., Hesjedal T., Pampuch C., Das A. K., Däweritz L., Koch R., Ploog K. H., Toliński T., Lindner J., Lenz K. and Baberschke K., *Phys. Rev. B*, **69** (2004) 081306(R).
[13] Guillaud C., *J. Phys. Radium*, **12** (1951) 223.
[14] Kittel C., *Phys. Rev.*, **120** (1960) 335.
[15] Bacon G. E. and Street R., *Nature*, **175** (1955) 518.
[16] Niranjan M. K., Sahu B. R. and Kleinman L., *Phys. Rev. B*, **70** (2004) 180406(R).
[17] Schippan F., Trampert A., Däweritz L. and Ploog K. H., *J. Vac. Sci. Technol. B*, **17** (1999) 1716.
[18] Kästner M., Herrmann C., Däweritz L. and Ploog K. H., *J. Appl. Phys.*, **92** (2002) 5711.
[19] Däweritz L., Ramsteiner M., Trampert A., Kästner M., Schippan F., Schönherr H.-P., Jenichen B. and Ploog K. H., *Phase Transition*, **76** (2003) 445.
[20] Ney A., Hesjedal T., Pampuch C., Mohanty J., Das A. K., Däweritz L., Koch R. and Ploog K. H., *Appl. Phys. Lett.*, **83** (2003) 2850.
[21] Weber M., Koch R. and Rieder K. H., *Phys. Rev. Lett.*, **73** (1994) 1166.
[22] Koch R., Das A. K., Yamaguchi H., Pampuch C., Ney A. and Ploog K. H., *J. Appl. Phys.*, **96** (2004) 2773.
[23] Koch R., Pampuch C., Yamaguchi H., Das A. K., Ney A., Däweritz L. and Ploog K. H., *Phys. Rev. B*, **70** (2004) 092406.
[24] Menyuk N., Kafalas J. A., Dwight K. and Goodenough J. B., *Phys. Rev.*, **177** (1969) 942.
[25] Chernenko V. A., Wee L., McCormick P. G. and Street R., *J. Appl. Phys.*, **85** (1999) 7833.
[26] Mira J., Rivadulla F., Rivas J., Fondado A., Guidi T., Caciuffo R., Carsughi F., Radaelli P. G. and Goodenough J. B., *Phys. Rev. Lett.*, **90** (2003) 097203.
[27] Ishikawa F., Koyama K., Watanabe K. and Wada H., *Jpn. J. Appl. Phys.*, **42** (2003) L918.
[28] Dörfler M. and Bärner K., *Phys. Status. Solidi (a)*, **17** (1973) 141.
[29] Lindner J., Toliński T., Lenz K., Kosubek E., Wende H., Baberschke A., Ney A., Hesjedal T., Pampuch C., Koch R., Däweritz L. and Ploog K. H., *J. Magn. & Magn. Mater.*, **277/1-2** (2004) 159.
[30] De Blois R. W. and Rodbell D. S., *Phys. Rev.*, **130** (1963) 1347.